Am J Physiol Endocrinol Metab 292: E1543–E1554, 2007.
First published January 30, 2007; doi:10.1152/ajpendo.00620.2006.

Protective role for nitric oxide during the endoplasmic reticulum stress response in pancreatic β-cells

Kajorn Kitiphongspattana,[1] Tarannum A. Khan,[2] Katrin Ishii-Schrade,[2] Michael W. Roe,[1] Louis H. Philipson,[1] and H. Rex Gaskins[2,3,4,5]

[1]*Department of Medicine, The University of Chicago, Chicago; and Departments of* [2]*Animal Sciences and* [3]*Pathobiology,* [4]*Division of Nutritional Sciences, and* [5]*Institute for Genomic Biology, University of Illinois at Urbana-Champaign, Urbana, Illinois*

Submitted 16 November 2006; accepted in final form 3 January 2007

Kitiphongspattana K, Khan TA, Ishii-Schrade K, Roe MW, Philipson LH, Gaskins HR. Protective role for nitric oxide during the endoplasmic reticulum stress response in pancreatic β-cells. *Am J Physiol Endocrinol Metab* 292: E1543–E1554, 2007. First published January 30, 2007; doi:10.1152/ajpendo.00620.2006.—Higher requirements for disulfide bond formation in professional secretory cells may affect intracellular redox homeostasis, particularly during an endoplasmic reticulum (ER) stress response. To assess this hypothesis, we investigated the effects of the ER stress response on the major redox couple (GSH/GSSG), endogenous ROS production, expression of genes involved in ER oxidative protein folding, general antioxidant defense, and thiol metabolism by use of the well-validated MIN6 β-cell as a model and mouse islets. The data revealed that glucose concentration-dependent decreases in the GSH/GSSG ratio were further decreased significantly by ER-derived oxidative stress induced by inhibiting ER-associated degradation with the specific proteasome inhibitor lactacystin (10 μM) in mouse islets. Notably, minimal cell death was observed during 12-h treatments. This was likely attributed to the upregulation of genes encoding the rate limiting enzyme for glutathione synthesis (γ-glutamylcysteine ligase), as well as genes involved in antioxidant defense (glutathione peroxidase, peroxiredoxin-1) and ER protein folding (*Grp78/BiP*, *PDI*, *Ero1*). Gene expression and reporter assays with a NO synthase inhibitor (N^{ω}-nitro-L-arginine methyl ester, 1–10 mM) indicated that endogenous NO production was essential for the upregulation of several ER stress-responsive genes. Specifically, gel shift analyses demonstrate NO-independent binding of the transcription factor NF-E2-related factor to the antioxidant response element Gclc-ARE4 in MIN6 cells. However, endogenous NO production was necessary for activation of Gclc-ARE4-driven reporter gene expression. Together, these data reveal a distinct protective role for NO during the ER stress response, which helps to dissipate ROS and promote β-cell survival.

endoplasmic reticulum-associated degradation; glutathione; proteasome

PANCREATIC β-CELLS EXHIBIT intrinsically low expression of the hydrogen peroxide-inactivating enzymes catalase, superoxide dismutase, and glutathione peroxidase and are thus particularly sensitive to oxidative and nitrosative stress (33, 58, 86). Therefore, glutathione (γ-glutamyl-L-cysteinyl-glycine, GSH), the major thiol redox buffer, may be especially important for β-cell antioxidant defense. In support of this possibility, intracellular GSH concentrations appear to vary in conjunction with β-cell sensitivity to insulin secretagogues (23, 26, 27, 52). Furthermore, high glucose concentrations increase intracellular concentrations of reactive oxygen species (ROS) in pancreatic islets (25, 26, 45, 46, 75, 84, 85, 92). Both mitochondrial and nonmitochondrial pathways are thought to contribute ROS to the glucotoxic process that impairs β-cell function (3–5, 25, 26, 32, 45, 46, 58, 71, 75, 77, 84–86, 92). Although multiple biochemical pathways and mechanisms of action have been implicated in the deleterious effects of chronic hyperglycemia and oxidative stress on the function of vascular, retinal, and renal tissues, less work has been done with pancreatic islets (25, 26, 38, 45, 46, 92).

The robust driving force for disulfide formation occurs by a protein relay involving endoplasmic reticulum (ER) oxidoreductin 1 (Ero1), a conserved FAD-dependent enzyme, and protein disulfide isomerase (PDI). Specifically, Ero1 is oxidized by molecular oxygen and in turn acts as a specific oxidant of PDI, which then directly oxidizes disulfide bonds in folding proteins. The transfer of electrons required for disulfide bond formation occurs via interactions between Ero1 and PDI in conjunction with GSH as a buffer (17, 27, 88). This process, referred to as "ER oxidation," contributes to reduction-oxidation (redox) homeostasis in the ER and enables proper folding of membrane and secretory proteins (17, 27, 88). However, the reduction of oxygen by Ero1 also produces ROS, particularly during an ER stress response (14, 38).

The enhanced generation of ROS during disulfide bond formation ["disulfide stress" (13, 58)] has particular relevance for pancreatic β-cells, which possess a highly developed ER. Recent data demonstrate that the degradation of misfolded proteins by the ubiquitin-proteasome pathway prevented ER-derived oxidative stress (38). However, relatively little is known about the effects of various pathologies associated with diabetes on thiol metabolism and quality control in the ER of the β-cell (36, 61, 70). Therefore, in the present study, we examined the effects of glucose and ER stress on the major redox couple (GSH/GSSG) in mouse islets and utilized the well-established MIN6 β-cell line as a model to assess the effects of ER stress induced by proteasome inhibition on the production of cellular ROS (and NO) and stability of the GSH/GSSG redox couple as well as molecular mechanisms regulating these processes. The data reveal a working model through which the β-cell may regulate redox homeostasis in response to ER stress.

MATERIALS AND METHODS

Chemical agents. The proteasome inhibitor lactacystin (LC) was purchased from Dr. E. J. Corey (Harvard University, Boston, MA).

Address for reprint requests and other correspondence: H. R. Gaskins, Univ. of Illinois, 1207 W. Gregory Dr., Urbana, IL 61801 (e-mail: hgaskins@uiuc.edu).

The costs of publication of this article were defrayed in part by the payment of page charges. The article must therefore be hereby marked "*advertisement*" in accordance with 18 U.S.C. Section 1734 solely to indicate this fact.

β-Mercaptoethanol (β-ME), *n*-acetyl-L-cysteine (NAC), N^{ω}-nitro-L-arginine methyl ester [L-NAME, a NO synthase (NOS) inhibitor], and tunicamycin (Tm) were obtained from Sigma (St. Louis, MO).

Mouse islet isolation and cell culture. Mouse islets were isolated from Hsd:ICR (CD-1) mice (Harlan, Indianapolis, IN) at 6–8 wk of age by use of a collagenase inflation method (32). Pancreatic inflations were performed with Hanks' balanced salt solution (HBSS; unless otherwise specified, cell culture reagents were purchased from Invitrogen Life Technologies, Grand Island, NY) containing 1.6 mg/ml collagenase P (Boehringer Mannheim, Mannheim, Germany), 4 μg/ml DNase I (Sigma), 9.2 mmol/l HEPES, 100 U/ml penicillin, and 100 μg/ml streptomycin. Islets were purified by centrifugation with a Histopaque gradient (1). Hand-picked islets were placed in Costar ultralow attachment polystyrene cluster plates (Corning Glass, Corning, NY). MIN6 cells were established from β-cell adenomas derived from transgenic mice harboring a hybrid rat insulin promoter-SV40 (simian virus 40) large T-antigen gene construct (37). MIN6 cells were maintained in 25 mM glucose-Dulbecco's modified Eagle's medium (DMEM) supplemented with Eagle's minimal essential medium nonessential amino acid supplement, 44 mM sodium bicarbonate, 15 mM HEPES, 10,000 U/ml penicillin plus 10,000 μg/ml streptomycin, 10% (vol/vol) heat-inactivated fetal bovine serum (FBS), 250 μl/ml Fungizone (containing 250 μg/ml amphotericin B and 250 μg/ml sodium deoxycholate). MIN6 cells and islets were maintained at 37°C in 95% air-5% CO_2. Experiments were performed when cells were ~70% confluent (passages 20–30) and after islets were precultured for 2 days in 5.6 mM glucose DMEM supplemented with 5% heat-inactivated FBS.

RNA extraction and cDNA synthesis. Total RNA was extracted with TRIzol reagent (Invitrogen, Grand Island, NY) from MIN6 cells treated in triplicate in the presence or absence of LC (10 μM, 4 h) or Tm (10 μg/ml, 4 h) with or without L-NAME (5–10 mM, 4 h). After quantification by spectrophotometry, equal quantities of RNA per treatment were reverse transcribed to cDNA using a GeneAmp PCR System 2400 thermocycler (Applied Biosystems, Foster City, CA) in a final reaction volume of 50 μl containing 1,000 ng of RNA, 10 μl of 5× PCR buffer, 1 mM $MgCl_2$, 40 μM dNTP, 1.25 μl RNAsin, 4 mM DTT, 1.25 μl of random hexamers, and 0.75 μl of MultiScribe reverse transcriptase from a GeneAmp Gold RNA PCR Core Kit (Applied Biosystems). The reaction cycle consisted of a 10-min incubation at 25°C followed by a 20-min incubation at 42°C, after which the cDNA was stored at 4 or −20°C.

Real-time quantitative RT-PCR. Quantitative RT-PCR analysis was performed in a GeneAmp 5700 Sequence Detection System (Applied Biosystems) in a final reaction volume of 25 μl containing SYBR Green PCR Master Mix (Applied Biosystems), 0.5 μl of (each) primer, and 5 μl of cDNA template. The primers used to detect *CHOP/Gadd153* (*Ddit3*, 397 bp), forward (5′-CAC ATC CCA AAG CCC TCG-3′) and reverse (5′-CTC AGT CCC CTC CTC AGC-3′); *Ero1-lα* (*Ero1l*; 202 bp), forward (5′-CGG GAT CCT GCG AGC TAC AAG TAT TC-3′) and reverse (5′-GGA ATT CGC CAC ATA CTC AGC ATC G-3′); *Ero1-lβ* (*Ero1lb*; 219 bp), forward (5′-CGG GAT CCC TTT TGT GAA CTT GAT GA-3′) and reverse (5′-GGA ATT CAG_CCA CGT ATA GAA TGA T-3′); *ERp61* (*Pdia3*, 223 bp), forward (5′-GTG CCT TCT CCA TAT GAA GT-3′) and reverse (5′-GGG TTT GTA GCT TCT CGT TG-3′); *Gapdh* (225 bp), forward (5′-GGA AGC TTG TCA TCA AC-3′) and reverse (5′-GGT GTG AAC CAC GAG AAA T-3′); *Gpx-1*, (120 bp), forward (5′-AAA A/GTG TGA G/CGT G/CAA TGG GC-3′) and reverse (5′-CTC CAA/T ATG ATG AGC TTG GG-3′); *Gclc* (336 bp), forward (5′-CTG YCC AAT TGT TAT GGC TT-3′) and reverse (5′-TCA AAM AGK GTS AGT GGG TC-3′); *Grp78/BiP* (*Hspa5*, 398 bp), forward (5′-CTG GGT ACA TTT GAT CTG ACT GG-3′) and reverse (5′-GCA TCC TGG TGG CTT TCC AGC CAT TC-3′); *PDI* (*Pdia3*, 186 bp), forward (5′-ACA GCT GGC AGG GAA GCT GA-3′) and reverse (5′-AGC CTC TGC TGC CAG CAA GA-3′); *Prx-1* (*Prdx1*, 470 bp), forward (5′-GTG GAT TCT CAC TTC TGT CAT CT-3′) and reverse (5′-GGC TTA TCT GGA ATC ACA CCA CG-3′). 18S ribosomal RNA (*Rn18s*, 137 bp) were forward (5′-CAT TCG AAC GTC TGC CCT ATC-3′) and reverse (5′-CCT GCT GCC TTC CTT GGA-3′); unspliced *Xbp-1* (*Xbp-1u* or *Nfx1*, 56 bp), forward (5′-CTG AGT CCG AAT CAG GTG CAG-3′) and reverse (5′-GTC CAT GGG AAG ATG TTC TGG-3′); spliced *Xbp-1* (*Xbp-1s*; 76 bp), forward (5′-CAG CAC TCA GAC TAT GTG CA-3′) and reverse (5′-GTC CAT GGG AAG ATG TTC TGG-3′). *Rn18s* or *Gapdh* expression was the constitutive control for determining relative RNA concentrations between samples and to confirm equal efficiency of the reverse transcription reactions. Serial dilutions of the template were prepared to verify that detection occurred in the linear range of amplification. All primers were previously validated in-house or by others (18, 24, 34, 41, 50, 66, 81). Standard curves generated for each primer set using MIN6 RNA as controls were used to calculate mRNA concentrations.

Quantification of endogenous ROS production. Oxidative activity was detected by flow cytometric analysis using the fluorescein-labeled dye dichlorodihydrofluorescein diacetate (H_2DCF, Molecular Probes). The acetoxymethyl ester derivative readily permeates cell membranes and is trapped within the cell after cleavage by esterases. Oxidation by ROS converts the dye from its nonfluorescent to its fluorescent form. In brief, cells were cultured with 10 μM H_2DCF for 30 min at 37°C (85). After incubation with the dye, cells were washed with PBS and dispersed with trypsin, and endogenous peroxides were measured with the EPICS XL-MCL flow cytometer controlled by SYSTEM II software (Beckman Coulter, Miami, FL). Fifty thousand events were recorded for each analysis. Results were calculated as the mean fluorescence intensity of treated relative to control cells.

Plate reader fluorometry. To characterize DAF-FM (4-amino-5-methylamino-2′,7′-difluorofluorescein) diacetete (NO-specific reagent, Molecular Probes) measurements of endogenous NO production and endogenous cNOS activity, plate reader fluorometry experiments were performed as described (83). In brief, plate fluorometry experiments were performed with 5×10^5 MIN6 cells/well in a 96-well plate by use of a SpectraMax Gemini microplate spectrofluorometer (Molecular Devices). MIN6 cells were loaded with 10 μM DAF-FM diacetate (in 2.8 mM glucose for 1 h) and exposed to glucose (2.8, 5.6, or 25 mM) in the presence or absence of LC (10 μM) or Tm (10 μg/ml) for 1 h, during which fluorescence measurements (495/515 nm) were taken every 36 s. Measurements were analyzed with SOFTmax Pro version 4.3.

GSH measurements and calculation of intracellular redox potential. Total GSH was derivatized with orthophthalaldehyde and measured by reverse-phase HPLC (as described previously in Ref. 54). To calculate the redox potential for the GSH/GSSG redox couple, the Nernst equation, $E_h = E_0 + RT/2F \ln([GSSG]/[GSH]^2)$, was used, in which R is the gas constant, T is the absolute temperature, and F is Faraday's constant (80). E_0 at pH 7.2 was 252 mV (19, 80). To determine GSH and GSSG concentrations, cell volume was estimated as 2 pl by a Beckman Coulter counter Model ZM.

Western blot analysis. MIN6 cells were treated in triplicate in the presence or absence of LC (10 μM, 4 h) or Tm (10 μg/ml, 4 h) and with or without L-NAME (5–10 mM, 4 h). Nuclear proteins and cytoplasmic proteins were extracted as described previously (80). Equal protein concentrations (15 μg) were size separated by 12% SDS-PAGE and transferred to nitrocellulose membranes. Blots were probed with a rabbit polyclonal anti-γ-GCLC (Lab Vision, Fremont, CA), rabbit polyclonal anti-Nrf2, goat polyclonal anti-lamin B, goat polyclonal anti-β-tubulin (Santa Cruz Biotechnology) and horseradish peroxidase-conjugated anti-mouse IgG, anti-goat IgG, or anti-rabbit IgG (Sigma). Bands were detected with the enhanced chemiluminescence (ECL) system (Amersham Biosciences, Piscataway, NJ). Immunoblots were scanned by optical densitometry to quantify the relative level of protein expression among treatments.

Apoptosis and cell viability by flow cytometry using Hoechst 33342 and propidium iodide double staining. Flow cytometric analysis was used to distinguish among normal, apoptotic, and necrotic cells stained with Hoechst 33342 and propidium iodide (PI) (9, 22). In brief, after cells were treated as indicated, a low concentration of Hoechst 33342 (1 mg/l, ~10^6 cells) was added to cells at 37°C for 3 min. By counterstaining with a viability stain, such as PI (1 mg/l), normal, apoptotic, and necrotic cells were distinguished. Ten thousand cells were analyzed, and apoptotic cells were identified as those with increased Hoechst 33342 fluorescence, low forward angle light scatter, and no PI fluorescence.

Measurement of intracellular ATP and ADP concentrations. ATP and ADP were determined as described previously (54). In brief, cells were washed twice with PBS, and an ice-cold, nitrogen-saturated precipitation solution (3 vol acetonitrile + 1 vol 10 mM KH_2PO_4, pH 7.4) was added to each well. Precipitation solution was made weekly, stored at 4°C, and sparged with nitrogen for 20 min prior to usage. Upon addition of precipitation solution, cells were harvested and transferred to an Eppendorf tube, vortexed, and centrifuged at 16,000 *g* for 4 min at 4°C. Ice-cold HPLC-grade chloroform (500 μl) was added to supernatants, vortexed for 60 s, and centrifuged at 16,000 *g* for 4 min at 4°C. Chloroform extraction of the aqueous phase was repeated twice, and samples were filtered through a 0.45-μm, 4-mm syringe filter and transferred to an autosampler vial. Samples (100 μl) were analyzed by HPLC immediately after sample preparation. HPLC separation was performed on a Waters 2695 separations module. Compounds were separated on a reverse-phase column (Kromasil C18, 5 μm, 250 mm × 4.6 mm) coupled to a guard column (Waters Symmetry C18, 5 μm, 20 mm × 3.2 mm) using tetrabutylammonium hydroxide as ion-pairing reagent. ATP and ADP were detected with a Waters 2487 dual-absorbance detector (260 nm). The detectors were connected in line. Peak areas were integrated using Millennium software version 3.2. Compound concentrations were calculated using standard curves.

Plasmids and constructs. The full-length cDNA clones encoding mouse Nrf2 (Clone ID 3663276) and mouse MafK (Clone ID 4189276) were purchased from Invitrogen. The coding region of Nrf2 cDNA was amplified by PCR using the primers GTG GTA CCA GCA TGA TGG ACT TGG AGT TGC C and ACT CGA GCT AGT TTT TCT TTG TAT CTG G containing *Kpn*I and *Xho*I restriction sites (underlined) and subcloned into vector pcDNA 3.1(+) to generate the construct pcDNA-Nrf2. The coding region of MafK was also amplified by PCR using the primers GGT AAG CTT GTT ATG ACG ACT AAT CCC AAG CC and AGA ATT CCT AGG AGG CGG CTG AGA AGG G containing *Hin*dIII and *Eco*RI restriction sites (underlined) and subcloned into the vector pcDNA3.1(+) to generate the construct pcDNA-MafK. The 6.5-kb mouse *Gclc* promoter-luciferase construct was a kind gift from Dr. Michael Rosenfeld (University of Washington, Seattle, WA) and has been described previously (8).

ARE4 gene reporter assays. MIN6 cells were seeded at a density of 2×10^5 per well in a 24-well plate. Forty-eight hours after seeding, cells were cotransfected using the Lipofectamine 2000 reagent (Invitrogen) with 1 μg of the mouse *Gclc* promoter-luciferase construct and 0.5 μg each of the pcDNA-Nrf2 and pcDNA-MafK constructs. 0.01 μg of the control plasmid pRL-TK encoding *Renilla* luciferase was included in each transfection to account for variability in transfection efficiency. Twenty-four hours after transfection, the medium was aspirated, and the cells were pretreated with medium without glucose for 1 h, after which it was replaced with medium containing 5.6 mM glucose ± L-NAME (10 mM). After 1 h, it was followed by treatment with or without 10 μM LC or Tm (10 μg/ml) for 8 h. Cell lysates were obtained using the passive lysis buffer (Promega), and luciferase activity was measured using the Dual Luciferase Reporter System (Promega), according to the manufacturer's instructions, on a Zylux FB12 luminometer. Luciferase activity from the reporter plasmid was normalized to that obtained from the *Renilla* luciferase, and the results are expressed as means ± SE of four independent experiments.

Nuclear extract preparation and electrophoretic mobility shift assay. Nuclear extracts from cells were prepared as described (80) and kept at −80°C until use. Protein content was measured using the Bradford method. The sequences of the oligonucleotides encompassed the ARE4 element (81) as follows: $ARE4_{wt}$ 5′-CCC CGT GAC TCA GCG CTT TGT-3′, $ARE4_{m2}$ 5′-CCC CGT GAC Ttg GCG CTT TGT-3′. $ARE4_{wt}$ was used as a positive control. Equimolar amounts of single-stranded oligonucleotides were annealed and radiolabeled using T4 polynucleotide kinase (Roche) and [γ-^{32}P]dATP (Amersham Biosciences). Radiolabeled probes were purified by gel filtration chromatography on mini Quick Spin Columns (Roche). Nuclear proteins (2.5–5 μg) were preincubated for 20 min on ice in 20 μl of binding buffer (20 mM Tris·HCl, pH 7.5, 50 mM NaCl, 5 mM $MgCl_2$, 1 mM DTT, 10% glycerol) with 1 μg of poly(dI-dC) (Roche). A radiolabeled DNA probe (5 fmol) was added, and the reaction was left for another 20 min on ice. For competition experiments, 1,000 × excess of the cold probe was added 20 min before the radiolabeled probe was added. To verify binding of Nrf2 and MafK to the ARE4 element, 1 μl of anti-Nrf2 (sc-722X) and/or anti-MafK antibody (sc-16872X; both from Santa Cruz Biotechnology) was added to the proteins and left for 30 min at room temperature before the radiolabeled probe was added. Samples were loaded onto a 6% nondenaturing polyacrylamide gel and subjected to electrophoresis as described. Gels were vacuum dried and autoradiographed for 2 to 48 h at −80°C.

RESULTS

Effects of glucose and ER stress on the GSH/GSSG redox couple in mouse islets and MIN6 cells. To examine the effects of glucose and ER stress on the redox state, islets were exposed to 2.8, 5.6, or 20 mM glucose in the absence or presence of proteasome inhibitor LC (10 μM) for 4 h. Intracellular GSH and GSSG concentrations were measured by HPLC and normalized on a per cellular DNA basis. Relative to the physiological 5.6 mM glucose treatment, total islet GSH concentrations were elevated ($P < 0.05$) in response to low and high glucose (2.8 mM and 20 mM, Fig. 1*A*). LC further increased the total GSH concentration in islets cultured in low glucose (2.8 mM). The GSH/GSSG ratio, indicative of redox status, revealed that islets became more oxidized in response to increasing concentrations of glucose. The GSH/GSSG ratio of islets cultured in 2.8 and 5.6 mM glucose decreased ($P < 0.05$) in response to LC, whereas this ratio was similar in control and LC-treated islets in the presence of high glucose (20 mM; Fig. 1*B*). Similar glucose effects on GSH/GSSG ratios were observed in MIN6 cells (data not shown).

To quantify intracellular redox state, the concentrations of GSH and GSSG in MIN6 cells treated with 25 mM glucose were used to calculate the intracellular GSH redox potential with the Nernst equation (78). Untreated control cells exhibited redox potentials similar to cells exposed to LC (10 μM) in 25 mM glucose for 4 but not 12 h of treatment [$E_h \approx -160$ mV, apoptotic range (78)]. Notably, exposure to LC for 4 h significantly decreased intracellular GSH concentrations, whereas 4-h exposure to Tm significantly increased intracellular GSH concentrations (Table 1). Supplementation with β-ME and NAC prevented ($P < 0.05$) the loss of intracellular GSH attributed to LC.

Measurements of endogenous ROS and NO production in MIN6 cells. Exposure of MIN6 cells to LC or Tm increased intracellular ROS concentrations (Fig. 2). The increase in

endogenous ROS was reduced by supplementation with β-ME (100 μM) or NAC (1 mM).

Endogenous cellular NO is synthesized by a family of NO synthase enzymes (reviewed in Ref. 51). To measure direct and dynamic endogenous NO production of the constitutive NOS activity in MIN6 cells, plate reader fluorometry experiments were performed (Fig. 3). In agreement with previous studies by Smukler et al. (83), endogenous NO production was proportional to increasing concentrations of glucose (2.8, 5.6 mM). However, the present data reveal that NOS activity was stimulated further by LC (10 μM). Tm (10 μg/ml) significantly increased endogenous NO production relative to untreated control cells in high glucose (25 mM). The NOS inhibitor L-NAME prevented endogenous NO production (data not shown). These results demonstrate that cultured β-cells produce NO in response to glucose and further implicate a role for NO during the ER stress response.

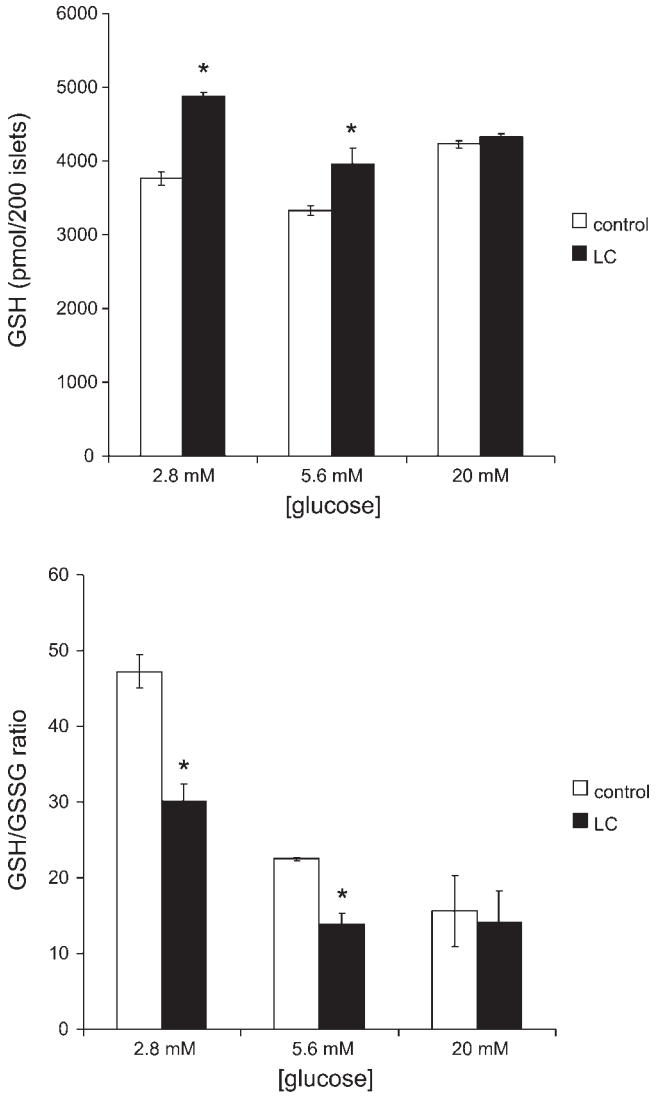

Fig. 1. Effects of glucose and endoplasmic reticulum (ER) stress on the GSH/GSSG redox couple in mouse islets. Mouse islets ($n = 3$, 200 islets/well) were treated with or without lactacystin (LC, 10 μM) in glucose (2.8, 5.6, 20 mM) for 4 h. After treatment, islets were collected, washed, and processed for GSH measurements as described in MATERIALS AND METHODS.

Table 1. *Quantification of intracellular redox potential in MIN6 cells with or without LC or Tm and in absence or presence of supplemental thiol antioxidants*

Treatments	GSH	GSSG	2GSH/GSSG Ratio	Mean E_h Value
Control	916±34	253.8±20.1	7.2	−185.0
LC	621.6±13.7*	165.6±4.9*	7.5	−180.3
LC + β-ME	989.6±24.5	266.4±38.2	9.7	−186.4
LC + NAC	781.2±13.2*	202±38.1	7.7	−183.8
Tm	1,386±48.4*	417.6±36.2*	6.6	−189.4
Tm + β-ME	2,120.4±6.9*	398.4±25.8*	10.6	−201.4
Tm + NAC	1,080±33.7	341.4±41.7	6.3	−185.4

Mean (±SE) concentrations of GSH and GSSG (pmol/mg DNA) are shown for MIN6 cells exposed for 4 h with or without lactacystin (LC, 10 μM) or tunicamycin (Tm, 10 μg/ml) and with or without supplemental thiol antioxidants β-mercaptoethanol (β-ME, 100 μM) or *n*-acetyl-L-cysteine (NAC, 1 mM). Intracellular redox potential (E_h value) was calculated using the Nernst equation based on previous estimates of cell volume and pH, as described in MATERIALS AND METHODS. Data are representative of 2 independent experiments. *$P < 0.05$ vs. control.

Fluorescence-activated cell sorting analysis of normal, apoptotic, and necrotic cells and cellular viability assessment. Normal, apoptotic, and necrotic cells were distinguished by double staining with Hoechst 33342 and PI (Table 2 and

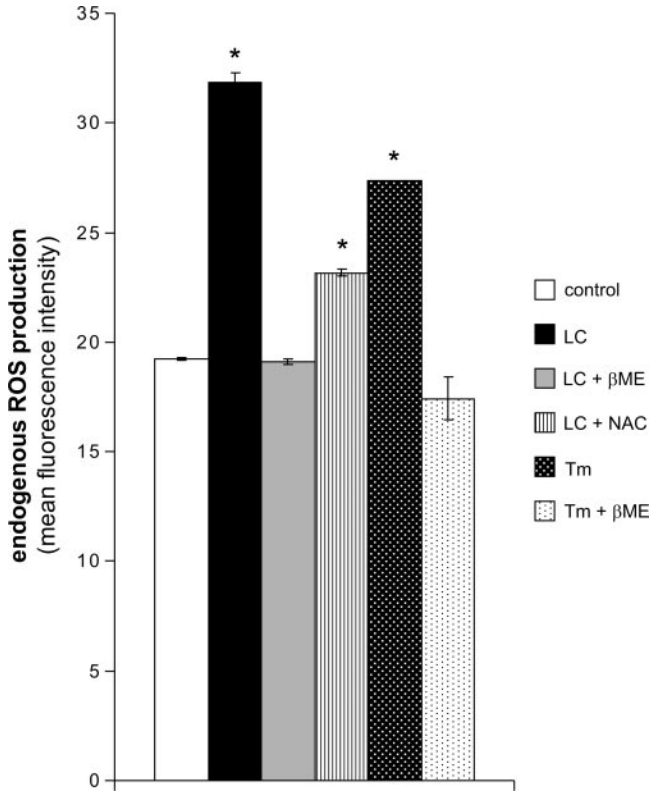

Fig. 2. Quantification of endogenous reactive oxygen species (ROS) production. MIN6 cells were treated with or without LC (10 μM, 4 h) or tunicamycin (Tm, 10 μg/ml, 4 h) with or without supplemental thiol antioxidants β-mercaptoethanol (β-ME) or *n*-acetyl-L-cysteine (NAC), rinsed with PBS, and incubated with the oxidative-sensitive probe dichlorodihydrofluorescein diacetate (H_2DCF, 10 μM) for 30 min after each treatment. Mean fluorescence intensity ± SE, which is directly proportional to endogenous ROS production, is shown for MIN6 cells treated with LC or Tm in the absence or presence of β-ME or NAC. *$P < 0.05$.

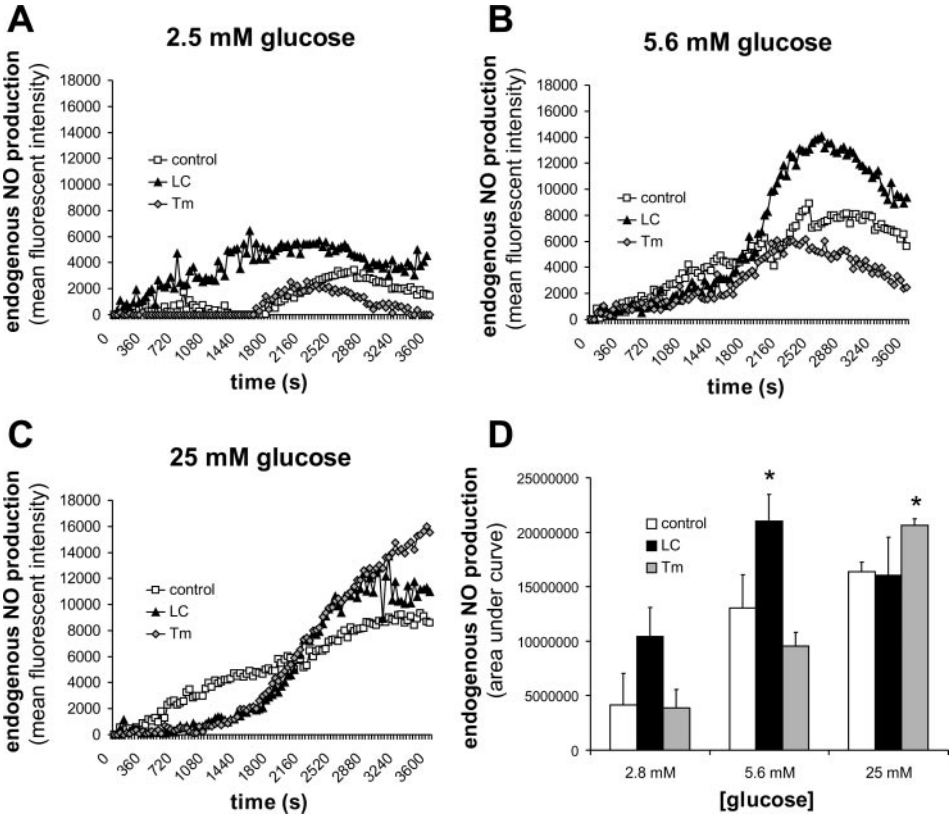

Fig. 3. Endogenous NO production in response to glucose stimulation and ER stress. MIN6 cells were loaded with DAF-FM diacetate (NO-specific reagent in 2.8 mM glucose for 1 h) and exposed to glucose (2.8, 5.6, 25 mM) with or without LC (10 μM) or Tm (10 μg/ml) for 1 h, during which measurements (495/515 nm) were recorded every 36 s. Representative graphs ($n = 4$) are shown for 3 independent experiments. *$P < 0.05$.

Refs. 9, 22). The number of Hoechst 33342- and PI-positive cells was quantified by fluorescence-activated cell sorting (FACS) analysis. The percentage of Hoechst 33342 and PI-positive cells was similar for MIN6 cells incubated in the absence or presence of LC (10 μM) or Tm (10 μg/ml) for 4 h. After a 12-h exposure to LC, the percentage of apoptotic and necrotic cells increased significantly relative to untreated cells in standard culture conditions (Table 2).

Enhanced expression of genes involved in oxidative protein folding in MIN6 cells. The formation of disulfide bonds in the ER requires PDI and ERO1, which reoxidizes PDI (60). To determine the effects of LC on *Ero1* and *PDI*, the mRNA concentrations of mouse *Ero1* homologs (*Ero1-lα* and *Ero1-lβ*), and two *PDI* enzymes (PDI and ERp61) were examined (Fig. 4). A significant increase in *Ero1-lα,* but not *Ero1-lβ* gene expression was observed in response to LC. The mRNA of both *PDI* family members (*PDI* and *ERp61*) were significantly increased in LC-treated MIN6 cells (Fig. 4).

Table 2. *FACS analysis of apoptotic and necrotic MIN6 cells ± lactacystin or tunicamycin*

	Control		Lactacystin		Tunicamycin	
	Apoptotic	Necrotic	Apoptotic	Necrotic	Apoptotic	Necrotic
4 h	3.4±0.6	3.2±0.1	4.6±1.2	2.1±0.2	3.3±0.2	4.2±0.4
12 h	2.0±0.4	3.5±0.4	5.1±1.1*	10.6±1.7*	3.6±0.8	6.8±0.3*

Percentage (means ± SE) of MIN6 apoptotic cells was measured by fluorescence-activated cell sorting (FACS) analysis after 4- and 12-h exposures to LC (10 μM) and Tm (10 μg/ml). Data are representative of 3 independent experiments. *$P < 0.05$, vs. control.

Effects of proteasome and NOS inhibition on expression of genes involved in thiol metabolism and antioxidant defense. To determine whether ER stress induced by LC (4 h, 10 μM) altered the expression of genes involved in thiol metabolism, mRNA expression of *Gclc* [encoding catalytic subunit of GCL, the rate-limiting enzyme for the synthesis of GSH (20, 39, 60, 65)], glutathione peroxidase, glutathione reductase, catalase, and manganese superoxide dismutase were examined. *Gclc* mRNA expression was below the detection limit for control MIN6 cells via standard RT-PCR. In contrast, *Gclc* mRNA transcripts were detected after exposure to LC and Tm (Fig. 5*A*). When the NOS inhibitor L-NAME (5 or 10 mM) was combined with LC (4 h, 10 μM) treatment, steady-state *Gclc* mRNA expression was similar to that of untreated controls. Quantitative PCR demonstrated that LC-induced *Gclc* mRNA expression was reduced significantly in response to L-NAME (5 mM; Fig. 5*B*). The protein expression of GCLC was similar among control and LC- and Tm-treated MIN6 cells (Fig. 5*C*). These data indicate that endogenous NO production or NOS activity contributes to the transcriptional upregulation of *Gclc* in MIN6 cells.

The mRNA expressions of glutathione reductase, catalase, and manganese superoxide dismutase were similar among control and LC- and Tm-treated MIN6 cells (data not shown). However, a significant increase in *Gpx-1* and *Prx-1* mRNA expression was observed in response to LC and Tm (Fig. 5*D*). When both the proteasome and NOS were inhibited, steady-state mRNAs of *Gpx-1* and *Prx-1* were lower ($P < 0.05$) or similar to untreated control mRNA (Fig. 5*D*). These data indicate that endogenous NO production or NOS activity

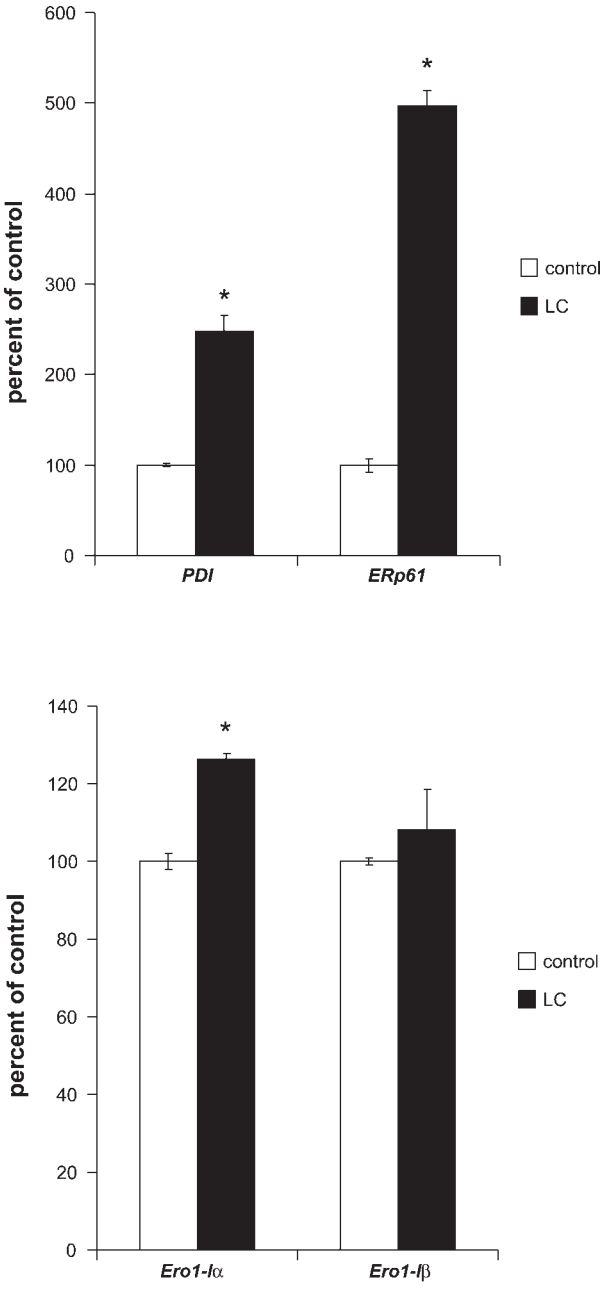

Fig. 4. Expression of genes involved in oxidative protein folding. Expressions of *Ero1-lα*, *Ero1-lβ*, *PDI*, and *ERp61* were determined by quantitative PCR. Open bars, control; filled bars, LC. $*P < 0.05$.

contributes to the transcriptional upregulation of *Gpx-1* and *Prx-1* in MIN6 cells.

To determine whether the transcriptional upregulation of an ER stress-responsive gene is dependent on endogenous NO production, mRNA expression of ER chaperone *GRP78/BiP* was examined by quantitative real-time RT-PCR in MIN6 cells treated with LC (10 μM) in the absence or presence of a NOS inhibitor (L-NAME, 10 mM) for 4 h (Fig. 5*D*). As expected, proteasome inhibition alone increased *Grp78/BiP* mRNA expression (Fig. 5*D*). When both the proteasome and NOS were inhibited, steady-state *Grp78/BiP* mRNA expression was lower ($P < 0.05$) or similar to that of untreated control cells (Fig. 5*D*).

Effects of proteasome and NOS inhibition on unfolded protein response activation and ER stress-responsive genes. Real-time quantitative RT-PCR was used to examine the activation of an unfolded protein response (UPR) in response to simultaneous proteasome and NOS inhibition in MIN6 cells. Transcription factor X-box-binding protein-1 (Xbp-1) is a regulator of the UPR (12, 41, 56, 94). On sensing misfolded proteins, an ER transmembrane endoribonuclease and kinase (Ire1) excises an intron from mammalian *Xbp-1* mRNA, resulting in the conversion of unspliced *Xbp-1 (Xbp-1u)* to spliced *Xbp-1* (*Xbp-1s*, 13, 42, 57, 94). The Xbp-1s then translocates to the nucleus where it binds its target sequence in the regulatory region of chaperone genes to induce their transcription. High expression of *Xbp-1s* relative to *Xbp-1u* is indicative of UPR activation (13, 42, 57, 94). Treatment of MIN6 cells with LC resulted in an accumulation of *Xbp-1s* mRNA and a concomitant decrease in *Xbp-1u* mRNA (Fig. 6). Inhibition of NOS did not alter this response.

The gene encoding C/EBP-homologous protein (CHOP), also known as growth arrest and DNA damage-inducible gene 153 (*Gadd153*), is a stress-inducible transcription factor that is activated by agents that adversely affect ER function (72). Expression of *CHOP/Gadd153* mRNA was detected by standard RT-PCR after exposure of MIN6 cells to LC (10 μM, 4 h) but not in untreated control cells (Fig. 7*A*). To determine whether *CHOP/Gadd153* induction was mediated by endogenous NO production, MIN6 cells were treated simultaneously with LC and NOS inhibitor L-NAME for 4 h. Induction of *CHOP/Gadd153* was not detected during simultaneous inhibition of proteasome and NOS. Quantitative PCR revealed that L-NAME decreased LC- and Tm-induced *CHOP/Gadd153* expression (Fig. 7*B*). These data indicate that endogenous NO production is necessary for the induction of *CHOP/Gadd153* in LC-treated MIN6 cells.

Constitutive nuclear localization of Nrf2. Nuclear localization of Nrf2 is essential for the transactivation of a variety of stress-responsive genes, including GCL (41, 81). Western blot analysis of nuclear and cytoplasmic extracts using anti-Nrf2 antibody revealed the accumulation of Nrf2 protein in the nucleus of LC-treated MIN6 cells (Fig. 8*A*). Inhibition of NOS did not significantly alter the localization of Nrf2. Nrf2 was not detected in the cytosol regardless of treatment. Lamin B and β-tubulin are shown as markers for nuclear and cytoplasmic compartments, respectively (Fig. 8*A*).

NOS inhibition prevented Gclc ARE4-mediated transactivation in ER-stressed MIN6 cells. Previous studies demonstrated Nrf and MafK transactivation of the *Gclc* promoter (21). To determine the role of NOS inhibition on ARE4-mediated gene expression, MIN6 cells were cotransfected with a mouse *Gclc* promoter-luciferase construct (1.0 μg) and 0.5 μg each of the pcDNA-Nrf2 and pcDNA-MafK constructs. Twenty-four hours after transfection, cells were treated with LC (10 μM) or Tm (10 μg/ml) in the absence or presence of L-NAME (10 mM) for 8 h in 5.6 mM glucose (Fig. 8, *B* and *C*). NOS inhibition repressed LC and Tm-induced activation of Gclc ARE4. These data further demonstrate an essential role for NO in regulating the Nrf2 pathway.

Electromobility shift assays demonstrate DNA binding of Nrf2 to ARE4 during UPR activation. To determine whether the binding of Nrf2 to an ARE is altered by UPR activation, electrophoretic mobility shift assays (EMSA) were performed.

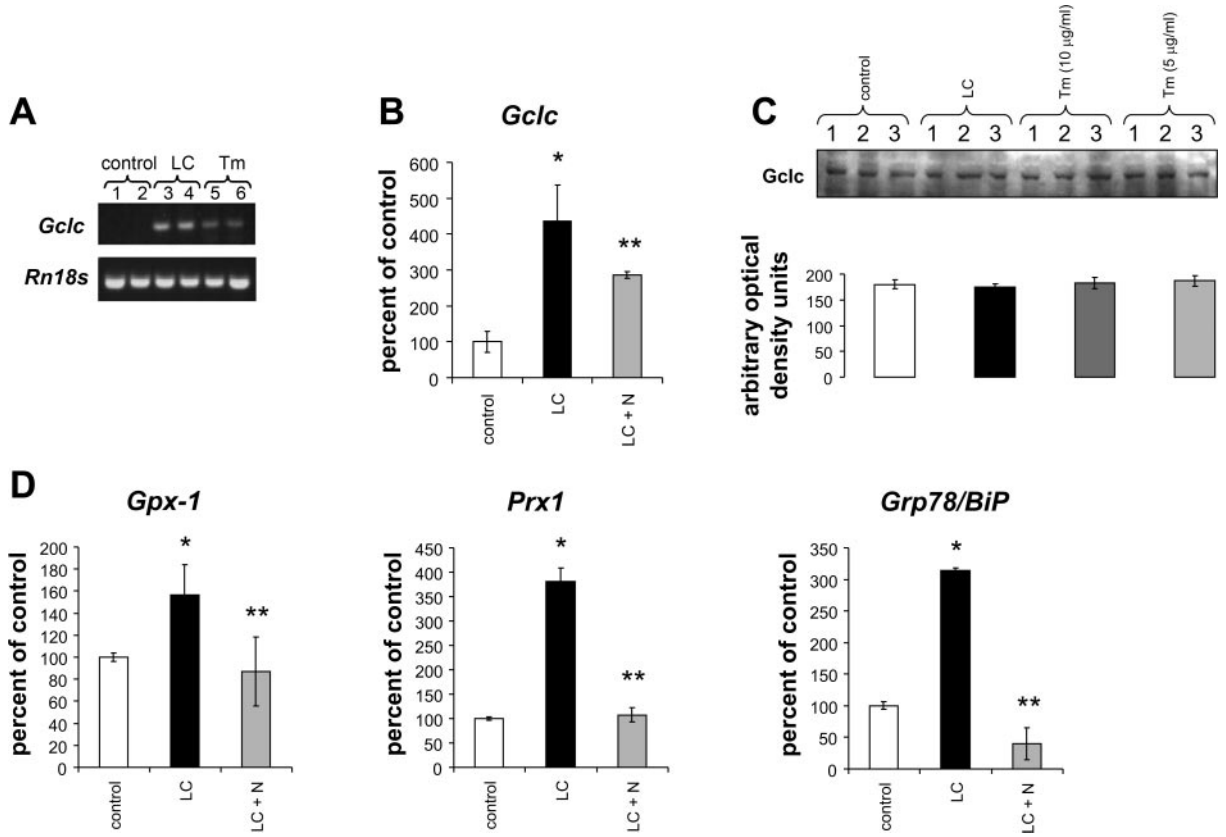

Fig. 5. Transcriptional upregulation of *Gclc* is decreased by NO synthase (NOS) inhibition. MIN6 cells were treated with LC (10 μM) with or without N^{ω}-nitro-L-arginine methyl ester (L-NAME, 10 mM) in 5.6 mM glucose for 4 h. After treatment, cells were washed with PBS, and protein or RNA was isolated. *A*: ethidium bromide-stained agarose gel. *B*: quantitative PCR (*Gclc* per *Gapdh*) demonstrated that NOS inhibition (5 mM L-NAME) downregulated LC-induced *Gclc* gene expression. Correctly sized RT-PCR products for *Gclc* (346 bp), and *Rn18s* (137 bp, constitutive control) are shown. *C*: Western blot analysis shows that Gclc protein expression was unaffected by LC or Tm treatment. Open bars, control; filled bars, LC; gray bars, Tm. *D*: quantitative PCR demonstrated that NOS inhibition repressed LC-mediated upregulation of genes involved in ER protein folding (*Grp78/BiP*), thiol metabolism (cellular glutathione peroxidase, *Gpx-1*), and antioxidant defense (peroxiredoxin-1, *Prx1*). MIN6 cells were treated with LC (10 μM) with or without L-NAME (N, 10 mM) in 5.6 mM glucose for 1 h. After treatment, cells were washed with PBS, and protein or RNA was isolated. Representative data are per *Rn18s* and from 1 of 3 independent experiments performed in triplicate are shown; means ± SE. $^{*}P < 0.05$, LC vs. control; $^{**}P < 0.05$, LC vs. LC + N.

ER stress induced by LC or Tm enhanced the binding of nuclear factors to the *Gclc* ARE4 [Fig. 8*D*, *lane 2* (control) vs. *lanes 4* (LC) and *6* (Tm)]. To determine whether Nrf2 and MafK are involved in ARE4 binding, band shift reactions were incubated for 1 h with anti-Nrf2 and anti-MafK antibodies. For each treatment, incubation with a mixture of anti-Nrf2 and anti-MafK antibodies disrupted ARE4 DNA binding activity (Fig. 8*D*, *lanes 3, 5,* and *7* relative to *lanes 2, 4,* and *6*, respectively). A similar EMSA was performed with each antibody separately. Anti-Nrf2 (Fig. 8*E*, *lane 3*), but not anti-MafK (Fig. 8*E*, *lane 4*) disrupted binding of the Nrf2-MafK complex to the *Gclc* ARE4. This observation may be explained by the fact that the anti-Nrf2 reagent used is directed against the COOH terminus of Nrf2, which includes the DNA

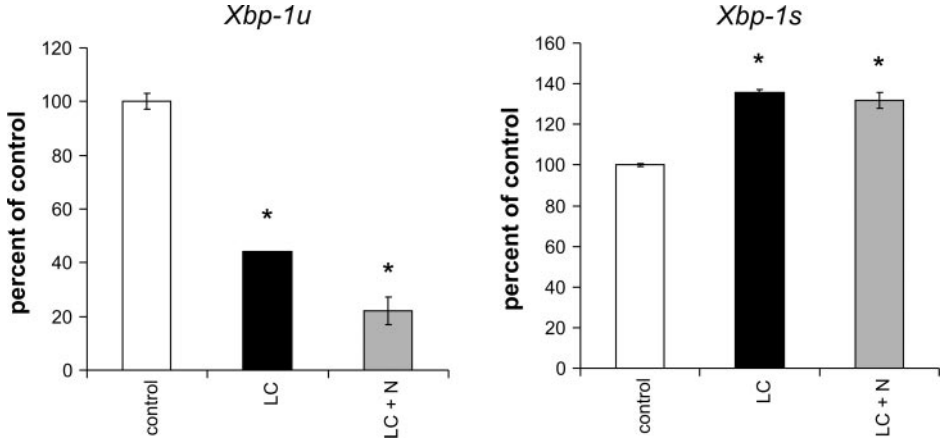

Fig. 6. Effects of proteasome and NOS inhibition on unfolded protein response activation. MIN6 cells were treated with LC (10 μM) with or without L-NAME (10 mM) in 5.6 mM glucose for 1 h. After treatment, cells were washed with PBS, and RNA was isolated. The relative steady-state active, spliced form of *Xbp-1* (*Xbp-1s*) and unspliced *Xbp-1* (*Xbp-1u*) per *Rn18s*, as determined by quantitative PCR, are shown. $^{*}P < 0.05$.

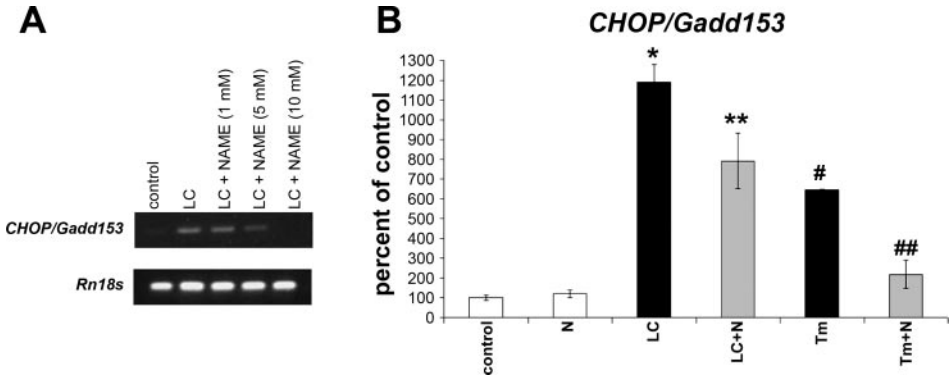

Fig. 7. Induction of *CHOP/Gadd153* is repressed by NOS inhibition. MIN6 cells were treated with LC (10 μM) or Tm (10 μM) with or without NOS inhibitor L-NAME (1, 5, 10 mM) in 5.6 mM glucose for 4 h. After treatment, cells were washed with PBS, and RNA was isolated. *A*: ethidium bromide-stained agarose gel demonstrates that *CHOP/Gadd153* was not induced when LC was incubated with L-NAME (10 mM). Correctly sized RT-PCR products for *CHOP/Gadd153* (397 bp), and *Rn18s* (137 bp, constitutive control) are shown. *B*: quantitative PCR revealed that L-NAME (N) decreased LC- or Tm-induced *CHOP/Gadd153* expression. Representative data from 1 of 3 independent experiments performed in triplicate are shown; means ± SE per *Gapdh*. $*P < 0.05$, LC vs. control; $**P < 0.05$, LC vs. LC + N; $\#P < 0.05$, Tm vs. control; $\#\#P < 0.05$, Tm vs. Tm + N.

binding domain. NOS inhibition did not significantly alter the binding of the Nrf2-MafK complex to the *Gclc* ARE4 induced by LC and Tm (data not shown).

DISCUSSION

The present studies investigated the effects of an ER stress response on the major redox couple (GSH/GSSG), endogenous ROS production, expression of genes involved in ER oxidative protein folding, general antioxidant defense, and thiol metabolism using mouse islets and the well-validated MIN6 β-cell line as a model system. Although the ER stress response is vital to ensure quality control, it also enhances the endogenous production of ROS, formed as byproducts during oxidative protein folding in the ER.

A glucose concentration-dependent decrease in the GSH/GSSG ratio was observed in islets after 4-h exposure to increasing concentrations of glucose (2.8, 5.6, 20 mM). Glucose itself may be an ER stressor through its ability to stimulate insulin synthesis and increase the number of proteins with disulfide bonds that must be folded properly in the ER lumen. To accommodate newly synthesized ER client proteins, the ER environment may adapt acutely through induction of a UPR. Persistent exposure to high glucose may lead to chronic UPR activation, (i.e., ERO1 and PDI expression) and thereby increase endogenous ROS production and redox signaling during high insulin demand. In agreement, constitutive expression of *Ero1-lβ* transcripts observed in professional secretory cells likely reflect their higher requirements in disulfide bond formation (27).

The physiological status of eukaryotic cells correlates with the redox potential (E_h value) of the GSH/GSSG couple (78). For example, the E_h value is most negative during proliferation and becomes more positive as cells differentiate (78). The present data demonstrate that MIN6 β-cells maintained a redox potential of approximately −185 mV. Relative to other confluent or differentiated cell lines [fibroblasts, HT-29 (78)], this E_h value is more oxidized and likely reflects the highly developed β-cell ER and its respective vital metabolic and secretory activities. Additionally, β-cells are also more sensitive to oxidative and nitrosative stress due to their intrinsically low expression of antioxidant enzymes (57, 71, 86).

It was suggested recently that the same pathways used in the activation of glucose-dependent insulin secretion (increased glycolytic flux, ATP-to-ADP ratio, and intracellular Ca^{2+} concentration) can dramatically enhance ROS production and manifestations of oxidative stress and, possibly, apoptosis (29). Indeed, it is generally acknowledged that ROS are byproducts of mitochondrial aerobic metabolism. However, in the present studies, the specific metabolic consequences of ER oxidation are highlighted as a contributor of endogenous ROS. We hypothesize that "ER oxidation" (also referred to as disulfide stress) generates excessive endogenous ROS, which contributes to the chronic oxidative stress observed in pancreatic β-cells during hyperglycemia. Our data revealed a glucose concentration-dependent decrease in the GSH/GSSG ratio, which was further decreased (i.e., oxidized) with ER stress in mouse islets. Notably, the maximal effects of ER oxidation were observed only in mouse islets stimulated with lower (2.8 or 5.6 mM) glucose concentrations. In high glucose (20–25 mM), the GSH/GSSG ratio was similar in ER-stressed and untreated control mouse islets and MIN6 cells. These data indicate the importance of determining the relative contributions of ROS generated from mitochondrial vs. ER metabolism. Specifically, the extent to which ER-derived ROS may contribute to the chronic oxidative stress observed in β-cells during hyperglycemia is unclear.

Persistent ER stress eventually leads to cell death (27, 36, 48, 67, 71), which may be attributed to excessive ROS. In agreement, prolonged ER stress (12 h) correlated with a significant decrease in the GSH/GSSG ratio that was not prevented by supplemental thiol antioxidants (data not shown). However, after 4 h of treatment with lactacystin or tunicamycin, the percentage of apoptotic and necrotic cells combined did not differ significantly from control cells and reached only 15% of total cells after 12 h of treatment. Upregulation of the rate-limiting enzyme for GSH synthesis (*Gclc*) and genes involved in antioxidant defense (*Gpx-1*, *Prx-1*) likely contributed to the maintenance of β-cell redox homeostasis and cell survival during this acute period.

The extent to which increased endogenous ROS production or enhanced redox signaling may contribute to cell survival during the ER stress response in β-cells is questionable. NO is

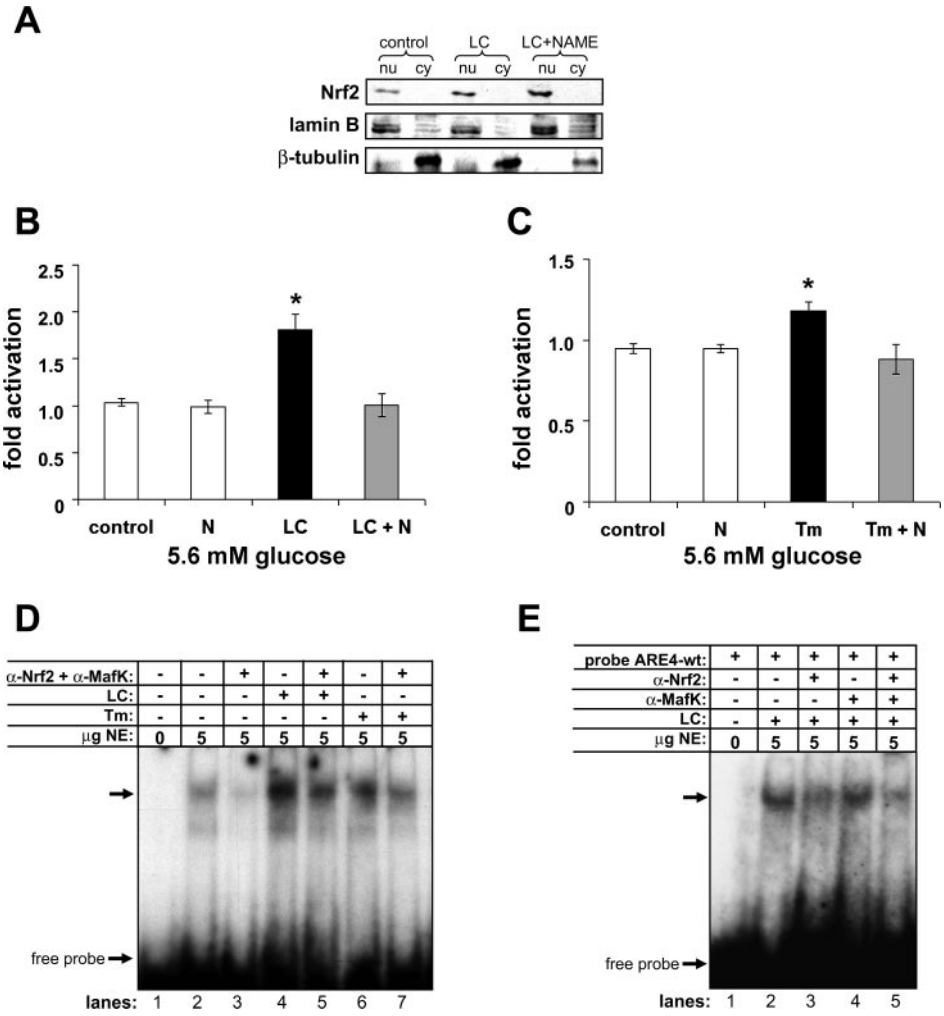

Fig. 8. Effects of NOS inhibition on antioxidant response element (ARE)4-mediated gene expression in ER-stressed MIN6 cells. *A*: nuclear localization of Nrf2 in response to ER stress. MIN6 cells were grown on 6-well plates and treated with LC (10 μM) with or without L-NAME (10 mM) in 5.6 mM glucose for 4 h. After treatment, cells were washed with PBS, and nuclear and cytoplasmic extracts were prepared. Ten micrograms of the nuclear proteins (nu) or cytoplasmic proteins (cy) were loaded onto a 12% polyacrylamide gel, and Western blotting was performed with anti-Nrf2, anti-lamin B, and anti-β-tubulin antibodies. Lamin B and β-tubulin are shown as markers for nuclear and cytoplasmic proteins, respectively. *B* and *C*: NOS inhibition prevents induction of ARE4-mediated gene expression in ER-stressed MIN6 cells. MIN6 cells were cotransfected with mouse *Gclc* promoter-luciferase construct along with pcDNA-Nrf2 and pcDNA-MafK constructs and pRL-TK plasmid encoding *Renilla* luciferase as an internal control. Twenty-four hours after transfection, cells were pretreated with medium without glucose for 1 h, after which it was replaced with medium containing glucose (5.6 mM, *B* and *C*) with or without L-NAME (N, 10 mM). After 1 h, cells were treated with or without LC (10 μM) or Tm (10 μM) for 8 h. Cell lysates were obtained and luciferase activities normalized against *Renilla* luciferase activity. Results are represented as means ± SE from 3 independent experiments. $*P < 0.05$. Electromobility shift assays demonstrate Nrf2 binding to ARE4. *D*: LC and Tm enhanced the binding of nuclear factors to the *Gclc* ARE4. The *Gclc* ARE4 was end labeled with [γ-^{32}P]ATP. Labeled $ARE4_{wt}$ probe (5 fmol) was incubated with nuclear extracts (NE, 5 μg) from MIN6 cells treated with LC (10 μM) or Tm (10 μg/ml) for 4 h and analyzed in a 6% nondenaturing polyacrylamide gel. Gels were dried and autoradiographed. *E*: in a similar experiment as in *D*, anti-Nrf2 and anti-MafK antibodies were incubated separately with nuclear extracts (*lanes 3* and *4*, respectively). ARE4 DNA binding activity was abrogated with unlabeled $ARE4_{m2}$ but not unlabeled oligonucleotides containing the m2 mutation ($ARE4_{m2}$, data not shown).

a signaling molecule that, in excess, causes cell death. Excessive NO exerts cytotoxic effects by reacting with superoxide and thereby generating the highly reactive free radical peroxynitrite, which causes nonspecific DNA, protein, and lipid damage (11). However, recent studies suggest that NO is also a potent antioxidant (reviewed in Ref. 73). Specifically, low NO concentrations produced by the constitutive NOS (cNOS) enzyme, which have been shown to regulate β-cell insulin release (2, 53, 69, 76, 79, 87, 89), may also terminate oxidative stress by *1*) suppressing iron-induced generation of hydroxyl radicals (·OH) via the Fenton reaction, *2*) interrupting the chain reaction of lipid peroxidation, *3*) augmenting the antioxidative potency of reduced GSH, and *4*) inhibiting cysteine proteases. The present data reveal that endogenous NO production or cNOS activity was enhanced by ER stress. Furthermore, inhibition of cNOS by L-NAME repressed the ER stress-induced expression of genes involved in thiol metabolism, antioxidant defense, and ER protein folding (*Gclc*, *Prx-1*, *Gpx-1*, *Grp78/BiP*). These data indicate that endogenous NO is vital for induction of antioxidant defense genes and those involved in ER protein folding in the β-cell.

The protective effects of NO in β-cells may be mediated by activation of Nrf2. Nrf2 is a critical transcription factor that binds to the ARE in the promoter region of a number of genes

encoding for antioxidant and phase 2 enzymes in numerous tissues and cell types (40, 68). However, to our knowledge, it has not been previously reported whether Nrf2 signaling controls the coordinated expression of antioxidant pathways and phase 2 enzymes in pancreatic β-cells. Our data demonstrate that inhibition of NO production did not prevent Nrf2 binding to the ARE. This observation suggests that Nrf2 may be constitutively localized to the nucleus of β-cells or implicates the existence of a NO-independent pathway for nuclear localization and activation of Nrf2. The present data support the former possibility in that Nrf2 was detected primarily in the nucleus in both control and treated cells. However, recent reports showed that PERK-dependent activation of Nrf2 contributes to redox homeostasis and cell survival following ER stress (15, 16). Therefore, independently of endogenous NO production, PERK may activate Nrf2. The potential redundancy of this pathway underscores the importance of maintaining redox homeostasis in pancreatic β-cells. Indeed, recent studies indicate that Nrf2 activation involves a coordinated process and is regulated at multiple levels (reviewed in Ref. 16). The present data demonstrate that cNOS inhibition repressed *Gclc* expression and ARE4 promoter activity despite UPR (and PERK) activation. In this regard, although NO-independent pathways for initiating the nuclear localization of Nrf2 exist, endogenous NO production is necessary for ultimately enhancing *Gclc* expression during the ER stress response. In agreement, NO-induced transcriptional upregulation of protective genes by Nrf2 via the ARE counteracts apoptosis in neuroblastoma cells (21). This and the present findings support the involvement of a NO-dependent mechanism underlying redox homeostasis in β-cells.

β-Cell dysfunction resulting from oxidative or disulfide stress may reflect differential genetic or environmental regulation of ER stress responses. Consistent with this hypothesis is a report that describes an "integrated stress response" consisting of the UPR and further regulation of amino acid metabolism and resistance to oxidative stress (37). Furthermore, genetic differences in the constitutive ability to dissipate ROS correlated with differential inbred strain susceptibility or resistance to alloxan- and streptozotocin-induced diabetes (62–64).

Collectively, the present data indicate that oxidative protein folding machinery in the ER may generate excessive ROS that accumulate over time and contribute to chronic oxidative stress during hyperglycemic conditions. Accordingly, β-cells respond to disulfide stress by increasing the total glutathione pool, possibly to buffer the excessive ROS produced during the ER stress response. In addition to changes in thiol metabolism, β-cells possess the capacity to regulate their intracellular redox state via induction of antioxidant defense genes. These effects are, in part, mediated by enhanced redox signaling via NO.

ACKNOWLEDGMENTS

K. Ishii-Schrade is presently at the Graduate School of Pharmaceutical Sciences, University of Tokyo, Tokyo, Japan.

GRANTS

This work was supported by National Institute of Diabetes and Digestive and Kidney Diseases Grants DK-49192 (H. R. Gaskins), DK-68822 and DK-64162 (M. W. Roe). K. Kitiphongspattana was supported in part by a Ruth Kirschstein Institutional National Research Service Award 5T32 DK-59802 (Division of Nutritional Sciences, University of Illinois at Urbana-Champaign) and an American Diabetes Association Mentor-based Fellowship.

REFERENCES

1. **Ablamunits V, Elias D, Cohen IR.** The pathogenicity of islet-infiltrating lymphocytes in the non-obese diabetic (NOD) mouse. *Clin Exp Immunol* 115: 260–267, 1999.
2. **Alm P, Ekstrom P, Henningsson R, Lundquist I.** Morphological evidence for the existence of nitric oxide and carbon monoxide pathways in the rat islets of Langerhans: an immunocytochemical and confocal microscopical study. *Diabetologia* 42: 978–986, 1999.
3. **Ammon HP, Abdel-Hamid M, Rao PG, Enz G.** Thiol-dependent and non-thiol-dependent stimulations of insulin release. *Diabetes* 33: 251–257, 1984.
4. **Ammon HP, Mark M.** Thiols and pancreatic beta-cell function: a review. *Cell Biochem Funct* 3: 157–171, 1985.
5. **Ammon HP, Wahl MA.** The impact of thiols for insulin secretion. *Exp Clin Endocrinol* 93: 136–142, 1989.
6. **Aridor M, Balch WE.** Integration of endoplasmic reticulum signaling in health and disease. *Nat Med* 5: 745–751, 1999.
7. **Bast A, Wolf G, Oberbäumer I, Walther R.** Oxidative and nitrosative stress induces peroxiredoxins in pancreatic beta cells. *Diabetologia* 45: 867–876, 2002.
8. **Belloc F, Dumain P, Boisseau MR, Jalloustre C, Reiffers J, Bernard P, Lacombe F.** A flow cytometric method using Hoechst 33342 and propidium iodide for simultaneous cell cycle analysis and apoptosis determination in unfixed cells. *Cytometry* 17: 59–65, 1994.
9. **Bea F, Hudson FN, Chait A, Kavanagh TJ, Rosenfeld ME.** Induction of glutathione synthesis in macrophages by oxidized low-density lipoproteins is mediated by consensus antioxidant response elements. *Circ Res* 92: 386–393, 2003.
10. **Brownlee M.** The pathobiology of diabetic complications: a unifying mechanism. *Diabetes* 54: 1615–1625, 2005.
11. **Brune B, von Knethen A, Sandau KB.** Nitric oxide (NO): an effector of apoptosis. *Cell Death Differ* 6: 969–975, 1999.
12. **Buckley BJ, Marshall ZM, Whorton AR.** Nitric oxide stimulates Nrf2 nuclear translocation in vascular endothelium. *Biochem Biophys Res Commun* 307: 973–979, 2003.
13. **Calfon M, Zeng H, Urano F, Till JH, Hubbard SR, Harding HP, Clark SG, Ron D.** IRE1 couples endoplasmic reticulum load to secretory capacity by processing the XBP-1 mRNA. *Nature* 415: 92–96, 2002.
14. **Chakravarthi S, Jessop CE, Bulleid NJ.** The role of glutathione in disulphide bond formation and endoplasmic-reticulum-generated oxidative stress. *EMBO Rep* 7: 271–275, 2006.
15. **Cullinan SB, Diehl JA.** PERK-dependent activation of Nrf2 contributes to redox homeostasis and cell survival following endoplasmic reticulum stress. *J Biol Chem* 279: 20108–20117, 2004.
16. **Cullinan SB, Diehl JA.** Coordination of ER and oxidative stress signaling: the PERK/Nrf2 signaling pathway. *Int J Biochem Cell Biol* 38: 317–332, 2006.
17. **Cuozzo JW, Kaiser CA.** Competition between glutathione and protein thiols for disulphide-bond formation. *Nat Cell Biol* 1: 130–135, 1999.
18. **Demasi M, Shringarpure R, Davies KJA.** Glutathiolation of the proteasome is enhanced by proteolytic inhibitors. *Arch Biochem Biophys* 389: 254–263, 2001.
19. **Demaurex N.** pH Homeostasis of cellular organelles. *News Physiol Sci* 17: 1–5, 2002.
20. **Deplancke B, Gaskins HR.** Redox control of the transsulfuration and glutathione biosynthesis pathways. *Curr Opin Nutr Metab Care* 5: 85–92, 2002.
21. **Dhakshinamoorthy S, Porter AG.** Nitric oxide-induced transcriptional up-regulation of protective genes by Nrf2 via the antioxidant response element counteracts apoptosis of neuroblastoma cells. *J Biol Chem* 279: 20096–20107, 2004.
22. **Dive C, Gregory CD, Phipps DJ, Evans DL, Milner AE, Wyllie AH.** Analysis and discrimination of necrosis and apoptosis (programmed cell death) by multiparameter flow cytometry. *Biochim Biophys Acta* 1133: 275–282, 1992.
23. **Ellgaard L, Molinari M, Helenius A.** Setting the standards: quality control in the secretory pathway. *Science* 286: 1882–1888, 1999.
24. **Efrat S, Leiser M, Surana M, Tal M, Fusco-Demane D, Fleischer N.** Murine insulinoma cell line with normal glucose-regulated insulin secretion. *Diabetes* 42: 901–907, 1993.
25. **Evans JL, Goldfine ID, Maddux BA, Grodsky GM.** Oxidative stress and stress-activated signaling pathways: a unifying hypothesis of type 2 diabetes. *Endocr Rev* 23: 599–622, 2002.

26. **Evans JL, Goldfine ID, Maddux BA, Grodsky GM.** Are oxidative stress-activated signaling pathways mediators of insulin resistance and beta-cell dysfunction? *Diabetes* 52: 1–8, 2003.
27. **Fassio A, Sitia R.** Formation, isomerisation and reduction of disulphide bonds during protein quality control in the endoplasmic reticulum. *Histochem Cell Biol* 117: 151–157, 2002.
28. **Fleming JV, Fontanier N, Harries DN, Rees WD.** The growth arrest genes gas5, gas6, and CHOP-10 (gadd153) are expressed in the mouse preimplantation embryo. *Mol Reprod Dev* 48: 310–316, 1997.
29. **Fridlyand LE, Philipson LH.** Does the glucose-dependent insulin secretion mechanism itself cause oxidative stress in pancreatic beta-cells? *Diabetes* 53: 1942–1948, 2004.
30. **Gess B, Holfauer KH, Wenger RH, Lohaus C, Meyer HE, Kurtz A.** The cellular oxygen tension regulates expression of the endoplasmic oxidoreductase ERO1-Lalpha. *Eur J Biochem* 270: 2228–2235, 2003.
31. **Go YM, Gipp JJ, Mulcahy T, Jones DP.** H2O2-dependent activation of GCLC-ARE4 reporter occurs by mitogen-activated protein kinase pathways without oxidation of cellular glutathione or thioredoxin-1. *J Biol Chem* 279: 5837–5845, 2004.
32. **Gotoh M, Maki T, Kiyoizumi T, Satomi S, Monaco AP.** An improved method for isolation of mouse pancreatic islets. *Transplantation* 40: 437–438, 1985.
33. **Grankvist K, Marklund SL, Taljedal IB.** CuZn-superoxide dismutase, Mn-superoxide dismutase, catalase and glutathione peroxidase in pancreatic islets and other tissues in the mouse. *Biochem J* 199: 393–398, 1981.
34. **Hanahan D.** Heritable formation of pancreatic beta-cell tumours in transgenic mice expressing recombinant insulin/simian virus 40 oncogenes. *Nature* 315: 115–122, 1985.
35. **Harding HP, Calfon M, Urano F, Novoa I, Ron D.** Transcriptional and translational control in the mammalian unfolded protein response. *Annu Rev Cell Dev* 18: 575–599, 2002.
36. **Harding HP, Ron D.** Endoplasmic reticulum stress and the development of diabetes: a review. *Diabetes* 51: S455–S461, 2002.
37. **Harding HP, Zhang Y, Zeng H, Novoa I, Lu PD, Calfon M, Sadri N, Yun C, Popko B, Paules R, Stojdl DF, Bell JC, Hettmann T, Leiden JM, Ron D.** An integrated stress response regulates amino acid metabolism and resistance to oxidative stress. *Mol Cell* 11: 619–633, 2003.
38. **Haynes CM, Titus EA, Cooper AA.** Degradation of misfolded proteins prevents ER-derived oxidative stress and cell death. *Mol Cell* 15: 767–776, 2004.
39. **Huang CS, Chang LS, Anderson ME, Meister A.** Catalytic and regulatory properties of the heavy subunit of rat kidney gamma-glutamylcysteine synthetase. *J Biol Chem* 268: 19675–19680, 1993.
40. **Itoh K, Chiba T, Takahashi S, Ishii T, Igarashi K, Katoh Y, Oyake T, Hayashi N, Satoh K, Hatayama I, Yamamoto M, Nabeshima Y.** An Nrf2/small Maf heterodimer mediates the induction of phase II detoxifying enzyme genes through antioxidant response elements. *Biochem Biophys Res Commun* 236: 313–322, 1997.
41. **Itoh K, Wakabayashi N, Katoh Y, Ishii T, Igarashi K, Engel JD, Yamamoto M.** Keap1 represses nuclear activation of antioxidant responsive elements by Nrf2 through binding to the amino-terminal Neh2 domain. *Genes Dev* 13: 76–86, 1999.
42. **Iwakoshi NN, Lee AH, Glimcher LH.** The X-box binding protein-1 transcription factor is required for plasma cell differentiation and the unfolded protein response. *Immunol Rev* 194: 29–38, 2003.
43. **Jaiswal AK.** Nrf2 signaling in coordinated activation of antioxidant gene expression. *Free Radic Biol Med* 36: 1199–1207, 2004.
44. **Jonas JC, Sharma A, Hasenkamp W, Ilkova H, Patané G, Laybutt R, Bonner-Weir S, Weir GC.** Chronic hyperglycemia triggers loss of pancreatic beta cell differentiation in an animal model of diabetes. *J Biol Chem* 274: 14112–14121, 1999.
45. **Kajimoto Y, Kaneto H.** Role of oxidative stress in pancreatic beta-cell dysfunction. *Ann NY Acad Sci* 1011: 168–176, 2004.
46. **Kaneto H, Kajimoto Y, Miyagawa J, Matsuoka T, Fujitani Y, Umayahara Y, Hanafusa T, Matsuzawa Y, Yamasaki Y, Hori M.** Beneficial effects of antioxidants in diabetes: possible protection of pancreatic beta-cells against glucose toxicity. *Diabetes* 48: 2398–2406, 1999.
47. **Kaneto H, Xu G, Song KH, Suzuma K, Bonner-Weir S, Sharma A, Weir GC.** Activation of the hexosamine pathway leads to deterioration of pancreatic beta-cell function through the induction of oxidative stress. *J Biol Chem* 276: 31099–31104, 2001.
48. **Kaufman RJ.** Stress signaling from the lumen of the endoplasmic reticulum: coordination of gene transcriptional and translational controls. *Genes Dev* 13: 1211–1233, 1999.
49. **Kitiphongspattana K, Mathews CE, Leiter EH, Gaskins HR.** Proteasome inhibition alters glucose-stimulated (pro)insulin secretion and turnover in pancreatic β-cells. *J Biol Chem* 280: 15727–15734, 2005.
50. **Knaack D, Fiore DM, Surana M, Leiser M, Laurance M, Fusco-DeMane D, Hegre OD, Fleischer N, Efrat S.** Clonal insulinoma cell line that stably maintains correct glucose responsiveness. *Diabetes* 43: 1413–1417, 1994.
51. **Knowles RG, Moncada S.** Nitric oxide synthases in mammals. *Biochem J* 298: 249–258, 1994.
52. **Kretz-Remy C.** and Arrigo AP. *Gene expression and thiol redox state Methods Enzymol* 348: 200–15, 2002.
53. **Lajoix AD, Reggio H, Chardes T, Peraldi-Roux S, Tribillac F, Roye M, Dietz S, Broca C, Manteghetti M, Ribes G, Wollheim CB, Gross R.** A neuronal isoform of nitric oxide synthase expressed in pancreatic β-cells controls insulin secretion. *Diabetes* 50: 1311–1323, 2001.
54. **Lazzarino G, Amorini AM, Fazzina G, Vagnozzi R, Signoretti S, Donzelli S, Di Stasio E, Giardina B, Tavazzi B.** Single-sample preparation for simultaneous cellular redox and energy state determination. *Anal Biochem* 332: 51–59, 2003.
55. **Lee AS.** Mammalian stress response: induction of the glucose-regulated protein family. *Curr Opin Cell Biol* 4: 267–273, 1992.
56. **Lee AS.** The glucose-regulated proteins: stress induction and clinical applications. *Trends Biochem Sci* 26: 504–510, 2001.
57. **Lee K, Tirasophon W, Shen X, Michalak M, Prywes R, Okada T, Yoshida H, Mori K, Kaufman RJ.** IRE1-mediated unconventional mRNA splicing and S2P-mediated ATF6 cleavage merge to regulate XBP1 in signaling the unfolded protein response. *Genes Dev* 16: 452–466, 2002.
58. **Lenzen S, Drinkgern J, Tiedge M.** Low antioxidant enzyme gene expression in pancreatic islets compared with various other mouse tissues. *Free Radic Biol Med* 20: 463–466, 1996.
59. **Li K, Hein S, Zou W, Klug G.** The glutathione-glutaredoxin system in Rhodobacter capsulatus: part of a complex regulatory network controlling defense against oxidative stress. *J Bacteriol* 186: 6800–6808, 2004.
60. **Lu SC.** Regulation of glutathione synthesis. *Curr Top Cell Regul* 36: 95–116, 2000.
61. **Marciniak SJ, Ron D.** Endoplasmic reticulum stress signaling in disease. *Physiol Rev* 86: 1133–1149, 2006.
62. **Mathews CE, Graser RT, Savinov A, Serreze DV, Leiter EH.** Unusual resistance of ALR/Lt mouse beta cells to autoimmune destruction: role for beta cell-expressed resistance determinants. *Proc Natl Acad Sci USA* 98: 235–240, 2001.
63. **Mathews CE, Leiter EH.** Resistance of ALR/Lt islets to free radical-mediated diabetogenic stress is inherited as a dominant trait. *Diabetes* 48: 2189–2196, 1999.
64. **Mathews CE, Leiter EH.** Constitutive differences in antioxidant defense status distinguish alloxan-resistant and alloxan-susceptible mice. *Free Radic Biol Med* 27: 449–455, 1999.
65. **Meister A, Anderson Glutathione ME.** *Annu Rev Biochem* 52: 722–760, 1983.
66. **Miyazaki J, Araki K, Yamato E, Ikegami H, Asano T, Shibasaki Y, Oka Y, Yamamura K.** Establishment of a pancreatic beta cell line that retains glucose-inducible insulin secretion: special reference to expression of glucose transporter isoforms. *Endocrinology* 127: 126–132, 1990.
67. **Mori K.** Tripartite management of unfolded proteins in the endoplasmic reticulum. *Cell* 101: 451–454, 2000.
68. **Motohashi H, Yamamoto M.** Nrf2-Keap1 defines a physiologically important stress response mechanism. *Trends Mol Med* 10: 549–557, 2004.
69. **Nakata M, Yada T, Nakagawa S, Kobayashi K, Maruyama I.** Citrulline-argininosuccinate-arginine cycle coupled to Ca2+-signaling in rat pancreatic beta-cells. *Biochem Biophys Res Commun* 235: 619–624, 1997.
70. **Nardai G, Korcsmaros T, Papp E, Csermely P.** Reduction of the endoplasmic reticulum accompanies the oxidative damage of diabetes mellitus. *Biofactors* 12: 259–267, 2003.
71. **Oyadomari S, Araki E, Mori M.** Endoplasmic reticulum stress-mediated apoptosis in pancreatic beta-cells. *Apoptosis* 7: 335–345, 2002.
72. **Oyadomari S, Mori M.** Roles of CHOP/GADD153 in endoplasmic reticulum stress. *Cell Death Differ* 11: 381–389, 2004.
73. **Pryor WA, Houk KN, Foote CS, Fukuto JM, Ignarro LJ, Squadrito GL, Davies KJ.** Free radical biology and medicine: it's a gas, man! *Am J Physiol Regul Integr Comp Physiol* 291: R491–R511, 2006.

74. **Robertson RP, Harmon JS.** Diabetes, glucose toxicity, and oxidative stress: a case of double jeopardy for the pancreatic islet beta cell. *Free Radic Biol Med* 41: 177–184, 2006.
75. **Robertson RP, Harmon J, Tran PO, Tanaka Y, Takahashi H.** Glucose toxicity in beta-cells: type 2 diabetes, good radicals gone bad, and the glutathione connection. *Diabetes* 52: 581–587, 2003.
76. **Salehi A, Carlberg M, Henningson R, Lundquist I.** Islet constitutive nitric oxide synthase: biochemical determination and regulatory function. *Am J Physiol Cell Physiol* 270: C1634–C1641, 1996.
77. **Sato H, Kuriyama-Matsumura K, Siow RCM, Ishii T, Bannai S, Mann E.** Induction of cystine transport via system x-c and maintenance of intracellular glutathione levels in pancreatic acinar and islet cell lines. *Biochim Biophys Acta* 1414: 85–94, 1998.
78. **Schafer FQ, Buettner GR.** Redox environment of the cell as viewed through the redox state of the glutathione disulfide/glutathione couple. *Free Radic Biol Med* 30: 1191–1212, 2001.
79. **Schmidt HH, Warner TD, Ishii K, Sheng H, Murad F.** Insulin secretion from pancreatic B cells caused by L-arginine-derived nitrogen oxides. *Science* 255: 721–723, 1992.
80. **Schreiber E, Matthias P, Muller M, Schaffner M.** Rapid detection of octamer binding proteins with "mini-extracts", prepared from a small number of cells. *Nucleic Acids Res* 17: 6419, 1989.
81. **Sekhar KR, Soltaninassab SR, Borrelli MJ, Xu ZQ, Meredith MJ, Domann FE, Freeman ML.** Inhibition of the 26S proteasome induces expression of GLCLC, the catalytic subunit for gamma-glutamylcysteine synthetase. *Biochem Biophys Res Commun* 270: 211–217, 2000.
82. **Siman R, Flood DG, Thinakaran G, Neumar RW.** Endoplasmic reticulum stress-induced cysteine protease activation in cortical neurons: effect of an Alzheimer's disease-linked presenilin-1 knock-in mutation. *J Biol Chem* 276: 44736–44743, 2001.
83. **Smukler SR, Tang L, Wheeler MB, Salapatek AM.** Exogenous nitric oxide and endogenous glucose-stimulated β-cell nitric oxide augment insulin release. *Diabetes* 51: 2450–2460, 2002.
84. **Takahashi H, Tran PO, LeRoy E, Harmon JS, Tanaka Y, Robertson RP.** D-Glyceraldehyde causes production of intracellular peroxide in pancreatic islets, oxidative stress, and defective beta cell function via non-mitochondrial pathways. *J Biol Chem* 279: 37316–37323, 2004.
85. **Tanaka Y, Tran POT, Harmon J, Robertson RP.** A role for glutathione peroxidase in protecting pancreatic beta cells against oxidative stress in a model of glucose toxicity. *Proc Natl Acad Sci USA* 99: 12363–12368, 2002.
86. **Tiedge M, Lortz S, Drinkgern J, Lenzen S.** Relation between antioxidant enzyme gene expression and antioxidative defense status of insulin-producing cells. *Diabetes* 46: 1733–1742, 1997.
87. **Tsuura Y, Ishida H, Shinomura T, Nishimura M, Seino Y.** Endogenous nitric oxide inhibits glucose-induced insulin secretion by suppression of phosphofructokinase activity in pancreatic islets. *Biochem Biophys Res Commun* 252: 34–38, 1998.
88. **Tu BP, Weissman JS.** The FAD- and O(2)-dependent reaction cycle of Ero1-mediated oxidative protein folding in the endoplasmic reticulum. *Mol Cell* 10: 983–994, 2002.
89. **Umehara K, Kataoka K, Ogura T, Esumi H, Kashima K, Ibata Y, Okamura H.** Comparative distribution of nitric oxide synthase (NOS) in pancreas of the dog and rat: immunocytochemistry of neuronal type NOS and histochemistry of NADPH-diaphorase. *Brain Res Bull* 42: 469–478, 1997.
90. **Wang J, Takeuchi T, Tanaka S, Kubo SK, Kayo T, Lu D, Takata K, Koizumi A, Izumi T.** A mutation in the insulin 2 gene induces diabetes with severe pancreatic beta-cell dysfunction in the Mody mouse. *J Clin Invest* 103: 27–37, 1999.
91. **Wild AC, Gipp JJ, Mulcahy T.** Overlapping antioxidant response element and PMA response element sequences mediate basal and beta-naphthoflavone-induced expression of the human gamma-glutamylcysteine synthetase catalytic subunit gene. *Biochem J* 332: 373–381, 1998.
92. **Wu L, Nicholson W, Knobel SM, Steffner RJ, May JM, Piston DW, Powers AC.** Oxidative stress is a mediator of glucose toxicity in insulin-secreting pancreatic islet cell lines. *J Biol Chem* 279: 12126–12134, 2004.
93. **Xu W, Liu L, Charles IG, Moncada S.** Nitric oxide induces coupling of mitochondrial signalling with the endoplasmic reticulum stress response. *Nature Cell Biol* 6: 1129–1134, 2004.
94. **Yoshida H, Matsui T, Yamamoto A, Okada T, Mori K.** XBP1 mRNA is induced by ATF6 and spliced by IRE1 in response to ER stress to produce a highly active transcription factor. *Cell* 107: 881–891, 2001.